ESRF	**Experiment title:** Crystal Lattice Tilting and Twisting in Biomimetic Calcium Carbonate Thin Films	**Experiment number**: **HC-3140**
Beamline: ID13	**Date of experiment**: from: 12 Apr 2017 to: 15 Apr 2017	**Date of report**:
Shifts: 9	**Local contact(s)**: Tilman Grunewald	*Received at ESRF:*

Names and affiliations of applicants (* indicates experimentalists):

Dr Joseph Harris*

Universitaet Erlangen-Nurnberg Laboratory of Glass and Ceramics Department of Materials Science 3 Martensstrasse 5 DE - 91058 ERLANGEN

PD Dr. Stephan E. Wolf

Universitaet Erlangen-Nurnberg Laboratory of Glass and Ceramics Department of Materials Science 3 Martensstrasse 5 DE - 91058 ERLANGEN

Report

Biominerals employ crystallographic texture gradients as functional motifs for toughening protective mineralized body parts, e.g., in calcareous oyster shells **[1]**. These biogenic ceramics composed of crystalline calcium carbonate (typically calcite) form from nanoparticle assembly processes and via a shape-preserving **[2]** solid-amorphous to crystalline phase transformation. We established a biomimetic model system that mimics the genesis and transformation process and provides access to the unusual feature of aligned or tilted crystallite assembly into flat, pseudo-circular spherulites (10 μm thickness, 500 μm diameter) **[2]**.

It was the goal of this experiment at ID13 to collect multiple stress/strain maps of spherulites with both aligned and tilted crystallite lattices and expect to see differences in stress/strain based on locations of organic enrichment and crystallite orientation gradients. We aimed to provide experimental evidence for and a conceptual model of the interdependence between lattice distortions generated during the spherulitic phase transformation) and crystallite misorientaiton.

Experimental Details

X-ray diffraction experiments were conducted at the ESRF, ID13, Grenoble (France). A focused x-ray spot of 13 keV photon energy was created using a fixed curvature Kirkpatrick-Baez (KB) mirror system or a compound beryllium lens transfocator (CRL), resulting in a spot-size of 0.7 x 0.5 μm and 2.5 x 2 μm (HxV) respectively. 2D scattering patterns were recorded using a Dectris Eiger4M X detector with a sample-to-detector distance of 113.7 mm (CRL) or 131.6 mm (KB). A helium-flushed flight tube was employed to reduce air scattering. Samples were scanned 2D perpendicular to the incident X-ray beam with a continuous scanning scheme with 500 nm step size and varying exposure time. The data were integrated using pyFAI-based python scripts. Azimuthally integrated peaks were fitted with a pseudo-voigt function in home-written python functions. The azimuthal peak position was fitted by two Gaussians, spaced by 180°. Biomimetic films were prepared according to standard procedures (see **[2]**) in advance and thoroughly characterized. Due to varying reaction conditions, the biomimetic films were determined to contain variable amounts of polymer inclusions.

Results

Our obtained results show that already minor changes in the intracrystalline polymer content occluded within the film impact on the crystallographic texture. With increasing intracrystalline polymer fractions, we found a transition between texturally distinct subtypes of spherulites: straight vaterite, leafy vaterite, curved calcite, and straight calcite. With lower amounts of spherulite-occluded polymer, we observed a quite unrestricted transformation of the amorphous precursor to straight vaterite spherulites, growing along the (100) or (101) direction. At slightly elevated polymer concentrations, enrichment of intracrystalline polymer correlates with non-linear growth patterns invoked by non-crystallographic branching, giving rise to leaf-like vaterite patches growing along (004). For higher fractions of occluded polymer, a transition to calcite is observed. However, transformation to calcite creates a higher transformation stress build-up, which triggers autodeformation mechanisms **[3]**. Twisting and rotating calcite spherulites form (Fig. 1A top/blue). At high concentrations of incorporated polymers, straight calcite spherulites growing along (012) direction emerge (Fig. 1A, bottom/green). This unexpected behavior, i.e., higher inclusion rates but less autodeformation, implies a stress-relaxation mechanism unforeseen in autodeformation. Thus, intergranular occluded organic matrices may act as intergranular stress mediator that allows straight spherulite formation by distributing localized stress. A strain distribution analysis reflects distinct changes between straight and curved spherulites (see Figure 1B).

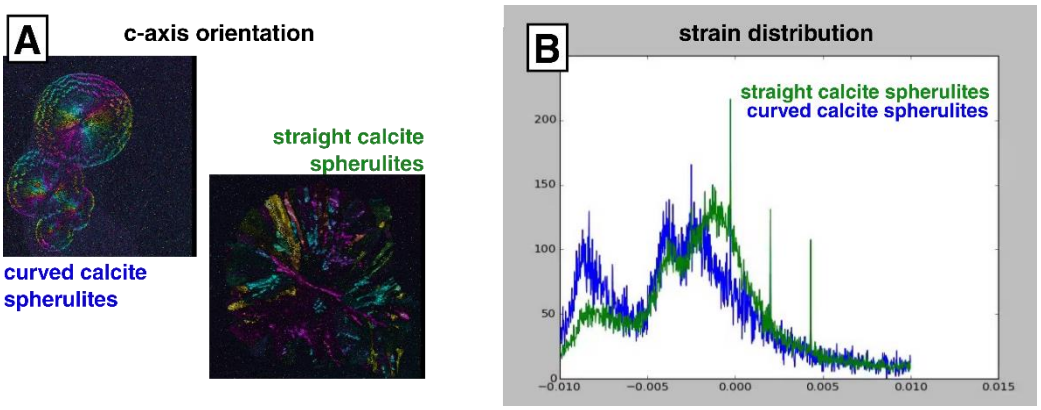

Figure 1. *Straight vs. curved spherulites.* ***A)*** *Orientation of the crystallographic growth axis of the spherulites. Color encodes orientation, saturation/hue the intensity/total scattered intensity.* ***B)*** *Unmixed strain distribution, extracted on basis of a geological refence.*

We calculated the orientation gradients and correlated them with strain to determine a pattern in the strain *vs.* gradient 2D histograms (Fig. 2). We found significant differences in the strain populations in three crystallographic directions. It is apparent that the strain in straight calcite spherulites is much less dependent on the orientation gradient than the strain of curved spherulites. The occurrence of two distinct stain populations in (012) is remarkable. For the c-axis strain, multiple but less pronounced and less clear demarcated strain populations are present. Similar strain analyses for vaterite spherulites reveal similar patterns. We currently perform further analyses to provide a mechanistic view of these results, i.a., by probing the stress state of the incorporated polymers spectroscopically supporting the unexpected stress-mediating action of higher polymer inclusions, in preparation for a final publication.

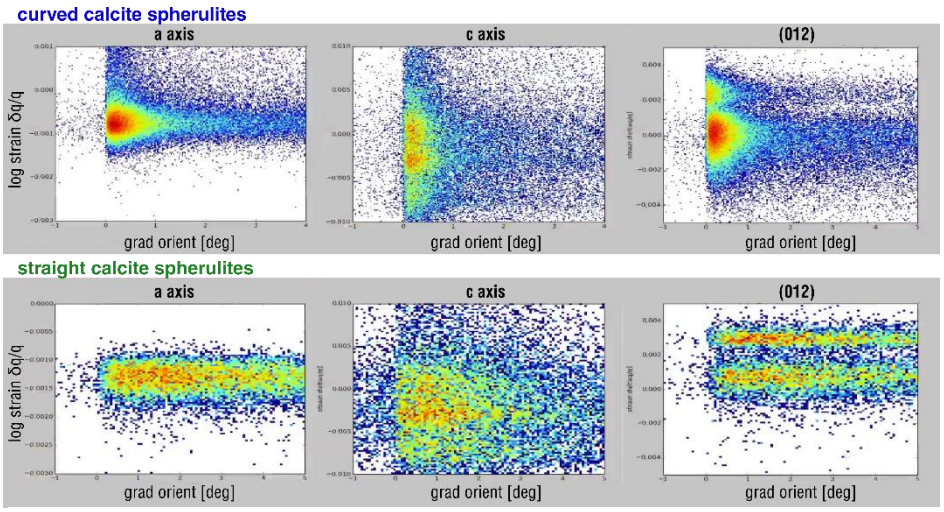

Figure 2. Strain/ orientation gradient correlations in curved (top) and straight bottom) spherulites.

References

[1] Wallis et al., Mater. Adv. 2022, 3 (3): 1527–38
[2] Harris et al., CrystEngComm 2015, 17 (36): 6831–37. Harris et al., Nanoscale Horizons 2019, 4: 1388–93.
[3] Shtukenberg& Kahr. Chemical Reviews 2012. 112 (3): 1805–38.